Eur. Phys. J. B **20**, 419–425 (2001)

**THE EUROPEAN PHYSICAL JOURNAL B**

EDP Sciences


# Next-nearest neighbor interaction and localized solutions of polymer chains

D. Hennig[a]

Freie Universität Berlin, Fachbereich Physik, Institut für Theoretische Physik, Arnimallee 14, 14195 Berlin, Germany

Received 4 October 2000

**Abstract.** We study localization in polymer chains modeled by the nonlinear discrete Schrödinger equation (DNLS) with next-nearest-neighbor (n-n-n) interaction extending beyond the usual nearest-neighbor exchange approximation. Modulational instability of plane carrier waves is discussed and it is shown that localization gets amplified under the influence of an enhanced interaction radius. Furthermore, we construct exact localized solitonlike solutions of the n-n-n interaction DNLS. To this end the stationary lattice system is cast into a nonlinear map. The homoclinic orbits of unstable equilibria of this map are attributed to standing solitonlike solutions of the lattice system. We note that in comparison with the standard next-neighbor interaction DNLS which bears only one type of static soliton-like states (either staggering or unstaggering) the one with n-n-n interaction radius can support unstaggering as well as staggering stationary localized states with frequencies lying above respectively below the linear band. Generally, the stronger the n-n-n interaction on the DNLS lattice the smaller are the maximal amplitudes of the standing solitonlike solutions and the less rapid are their exponential decays.

**PACS.** 63.20.Pw Localized modes – 63.20.Ry Anharmonic lattice modes – 63.20.Kr Phonon-electron and phonon-phonon interactions

## 1 The nonlinear discrete Schrödinger equation with long range interaction

The nonlinear Schrödinger equation (DNLS) has been successfully applied over the last years in modeling various physical systems. It found application in condensed matter systems, nonlinear optics, exciton motion in molecular crystals, electrical networks and for the dynamics of molecular vibrations [1]. Basic to this short range interaction DNLS (hereafter referred to as the standard DNLS) is a tight-binding system taking into account only the direct interaction between adjacent lattice sites. However, in some physical contexts the range of the interaction exceeds the radius of the nearest neighborhood so that each lattice site interacts with sites being more than one lattice unit apart from it too. To emphasize the physical importance of long range interaction we recall that the exciton transfer in molecular crystals and the transport of vibronic energy in biomolecules are mediated by dipole-dipole interaction with a typical long range power law dependence on the distance between the molecular subunits. In DNA molecules charged groups with Coulomb interaction are responsible for a long range interaction between them [2–6]. For excitons and photons in semiconductors and molecular aggregates the polariton effect leads a to long range interaction radius [2,3]. Finally, as a result of the stable secondary structure of $\alpha$-helix and $\beta$-sheet regions of proteins [4] protein electron transfer may proceed along one-dimensional pathways for which the exchange interaction includes besides the nearest neighbors also the next-nearest neighbors of peptide groups along a polypeptide chain.

There are only a few papers concerning the effects of long range interaction in nonlinear lattice dynamics [5–13] (and references therein).

The standard DNLS represents a Hamiltonian nonlinear lattice system for which the general existence of breather solutions, that is spatially localized but time-oscillating states, has been proven [14,15]. Such intrinsically localized states arise as the result of the interplay between lattice discreteness, nonlinearity and dispersive interactions and have attracted much interest over the past years (for a review see [16]). Specifically, for the standard DNLS the existence and stability of intrinsically localized mode have been considered in [17–22]. The scope of this paper is to investigate the impact of n-n-n interaction on the creation of localized solutions in the context of the DNLS.

We consider the nonlinear Schrödinger equation with long range interaction given by

$$\mathrm{i}\frac{\mathrm{d}c_n(t)}{\mathrm{d}t} + \gamma|c_n(t)|^2\, c_n(t) + \sum_{m=1}^{N} V_m(c_{n+m}(t) + c_{n-m}(t)) = 0. \quad (1)$$

The real parameter $\gamma \geq 0$ determines the nonlinearity strength and the $V_m$'s regulate the degree of the coupling

[a] e-mail: hennigd@physik.fu-berlin.de

between the lattice oscillators at sites $n$ and $n \pm m$. The long range interaction $V_{m\geq 1}$ serves as the extension of the standard DNLS lattice for which only nearest neighbor interaction were taken into account. In the limit of $V_m = 0$ for $|m| \geq 2$, equation (1) reduces to the standard DNLS system of short range interaction.

The paper is organized as follows: In Section 2 we discuss the stability of carrier plane wave solutions of the n-n-n interaction DNLS. The parameter space is searched for the occurrence of modulational instability. For n-n-n interaction radius the formation of localized pulses is demonstrated. The second part of the paper deals with the solution behavior of the stationary n-n-n interaction DNLS. The stationary system is interpreted as a nonlinear map in a four-dimensional phase space. The stability of the equilibrium point of this map located at the origin is examined. In the case of an unstable hyperbolic point it is shown that the construction of exact solitonlike lattice solutions can be achieved. These standing localized solutions are supported by homoclinic map orbits. Finally in Section 4 we give a brief summary.

## 2 Modulational instability

Nonlinear wave equations may exhibit modulational instability leading to a self induced modulation of an input plane wave with the subsequent generation of localized pulses. In this way energy localization in a homogeneous nonlinear system is possible and is manifested in the formation of envelope solitons [23–27]. Experimentally these results are confirmed by the observation of localized modes for example in electrical networks [28].

In the current section we explore the stability properties of equation (1) which possesses exact plane wave solutions

$$c_n(t) = c_0 \exp[\mathrm{i}(qn - \omega t)] \equiv c_0 \exp(\mathrm{i}\psi_n), \tag{2}$$

where $q$ is the wave number. The frequency $\omega$ satisfies the nonlinear dispersion relation

$$\omega = 2\sum_{n=1}^{N} V_n \cos(nq) + \gamma\, c_0^2. \tag{3}$$

To examine the linear stability of the solution (2) we use the ansatz $c_n(t) = (c_0 + b_n)\exp(\mathrm{i}\Theta_n + \mathrm{i}\psi_n)$ with the complex quantities $b_n$ being small in comparison to $c_0$. We derive the linear system for the dynamics of the perturbation

$$\begin{aligned} c_0\dot{\psi}_n = &-2\gamma c_0^2\, b_n + \sum_{m=1}^{N} V_m \left[(b_{n+m} + b_{n-m} - 2b_n)\cos(mq)\right. \\ &\left.-(\psi_{n+m} - \psi_{n-m})\sin(mq)\, c_0\right] \end{aligned} \tag{4}$$

$$\begin{aligned} \dot{b}_n = &\sum_{m=1}^{N} V_m \left[\cos(mq)(\psi_{n+m} + \psi_{n-m} - 2\psi_m)c_0\right. \\ &\left.+ (b_{n+m} - b_{n-m})\sin(mq)\right]. \end{aligned} \tag{5}$$

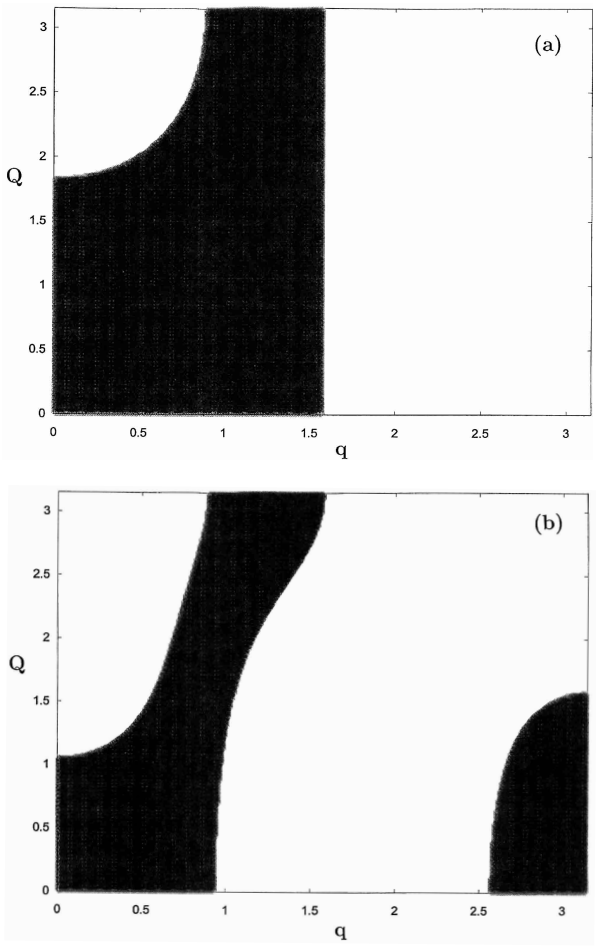


**Fig. 1.** Regions of modulational instability in the $q$-$Q$-plane indicated by the dark area(s). Parameters: $\gamma = 1$, $c_0 = 0.5$ and $b = 0.01$. (a) The standard DNLS with $V_1 = 0.2$. (b) The n-n-n DNLS with $V_1 = 0.2$ and $V_2 = 0.1$.

From the system (4) and (5) we deduce the dispersion relation for the perturbational wave

$$\begin{aligned} \left(\Omega + 2\sum_{m=1}^{N} V_m \sin(mq)\sin(mQ)\right)^2 &= 4\sum_{m=1}^{N} V_m \cos(mq) \\ \times \sin^2\left(\frac{mQ}{2}\right)&\left[4\sum_{m=1}^{N} V_m \cos(mq)\sin^2\left(\frac{mQ}{2}\right) - 2\gamma c_0^2\right], \end{aligned} \tag{6}$$

where $\Omega$ and $Q$ denote the corresponding frequency and wave number. The dispersion relation (6) enables to determine the parameter constellations $(q, Q)$ for which a carrier wave with wave number $q$ becomes unstable. In Figure 1 we show the regions of modulational instability on the $q$-$Q$-parameter plane for different interaction ranges.

The regions of modulational instability for the standard DNLS equation of $V_1 \neq 0$ and $V_{n\geq 2} = 0$ for which a given site $m$ is coupled only to its left and right adjacent neighboring sites $m \pm 1$ is depicted as the dark area in

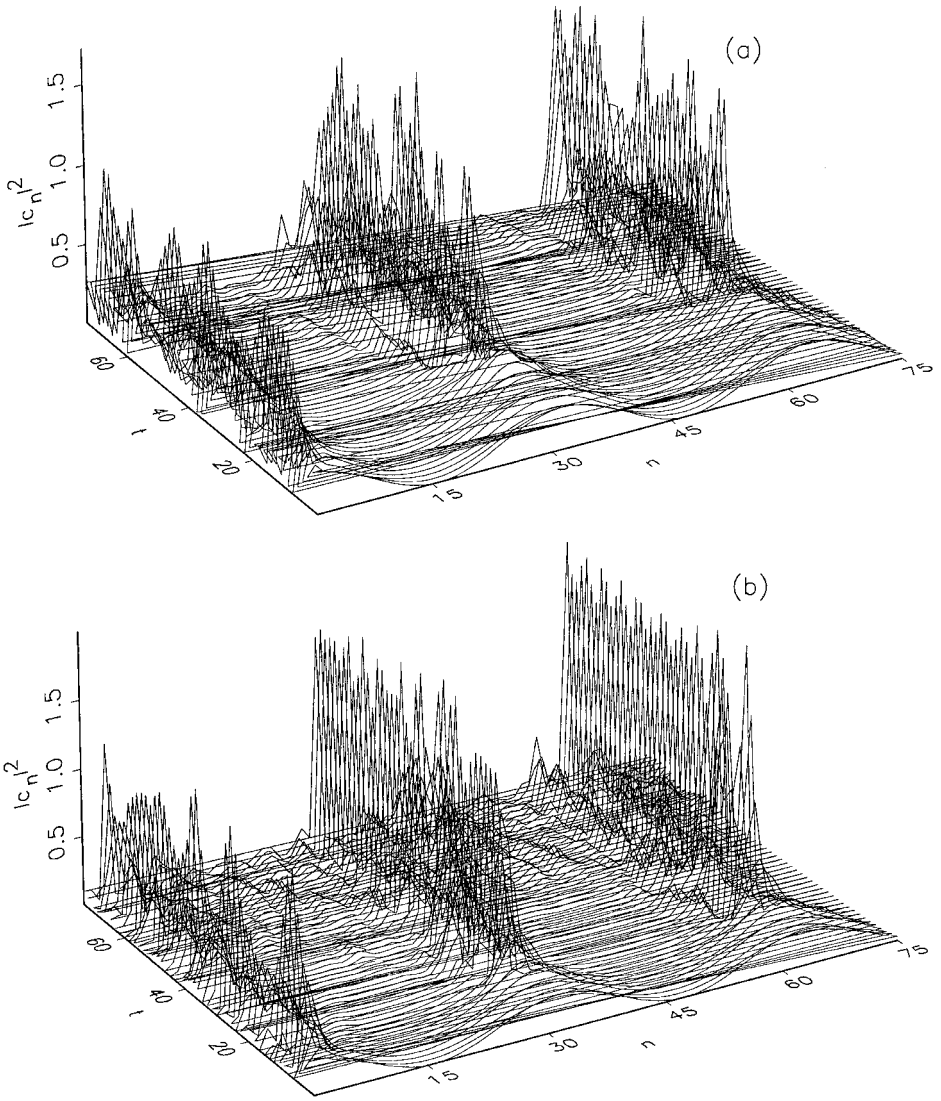


**Fig. 2.** Localized pulses on the DNSL lattice due to modulational instability demonstrating the rising degree of localization with extended interaction radius. (a) The standard DNLS: parameters as in Figure 1a and $q = Q = 0.5$. (b) The n-n-n DNLS: parameters as in Figure 1b and $q = Q = 0.5$.

Figure 1a. Figure 1b illustrates the parameter regions of modulational instability for n-n-n interaction with $V_1 \neq 0$, $V_2 \neq 0$ and $V_{n\geq 3} = 0$. In comparison with Figure 1a we note that for the extended interaction range the area in the $q$-$Q$-plane with $q \leq \pi/2$ for which modulational instability is possible shrinks. Especially, a large portion of the stripe $1 \lesssim q \leq \pi/2$ does no longer belong to the area of modulational instability and only the impact of modulations of large $Q$ remains in this wave number range. Additionally carrier waves with large wave numbers enter the region of modulational instability. Consequently, modulational instability is possible for high-frequency oscillations too. Thus two types of nonlinear localized modes exist with frequencies lying below (above) the linear band resulting in out-of-phase (in-phase) oscillations of neighboring lattice oscillators. (These localized modes have also been called staggered (unstaggered) soliton-like states [26].) A similar result was obtained in the case of a generalized deformable DNLS with nearest-neighbor interaction [27].

In Figure 2 we illustrate the influence of the interaction range on the formation of localized pulses in cause of modulational instability. The amplitude pattern $|c_n(t)|^2$ of the standard DNLS is shown in Figure 2a. The modulated carrier wave is initiated as $c_n(0) = (c_0 + b\cos(Qn))\cos(qn)$ with $c_0 = 0.5$ and $b = 0.01$. We recognize three separated localized pulses. Taking into account n-n-n interaction (Fig. 2b) leads to more pronounced degree of localization in the sense that not only the amplitudes of the localized pulses become larger but also their widths diminish. Similar results regarding modulational instability behavior were obtained for long-ranging interaction when the transfer matrix elements obey a distance dependence according to a power law (arising in the case of dipole-dipole interaction [6]). Obviously, with longer range

interaction the system's inherent length scale determined by the interaction radius, extends. In order to 'defeat' the resulting enhanced dispersion and to maintain localized solutions the lattice system responses by adapting its localized pulses to larger amplitudes.

## 3 Stationary localized solutions

We study stationary solutions of the system (1) which are obtained from the ansatz

$$c_n(t) = \phi_n \, \mathrm{e}^{\mathrm{i}\omega t} \tag{7}$$

with $\phi_n \in R$ and a rotation frequency $\omega$. Substituting (7) into (1) we obtain

$$\omega\phi_n = \gamma\phi_n^3 + \sum_{m=1}^{N} V_m(\phi_{n+m} + \phi_{n-m}). \tag{8}$$

Setting $x_n^{(N-k)} = \phi_{n+k}$ with $-N \leq k \leq N-1$ we express this difference system as a $2N$-dimensional map $\mathcal{M} : R^{2N} \longrightarrow R^{2N}$ determined by

$$x_{n+1}^{(1)} = \frac{1}{V_N}\left[\omega x_n^{(N)} - \gamma (x_n^{(N)})^3\right] - \frac{1}{V_N}\sum_{m=1}^{N} V_m (x_n^{(N+m)} + x_n^{(N-m)}) - x_n^{(2N)} \tag{9}$$

$$x_{n+1}^{(k+1)} = x_n^{(k)}, \qquad 1 \leq k \leq 2N-1, \tag{10}$$

with the condition $V_N \neq 0$. This map $\mathcal{M}$ is volume preserving because the Jacobian matrix $D\mathcal{M}$ fulfills the condition $\det D\mathcal{M} = 1$. Furthermore the map can be written as the product of two involutions $\mathcal{M} = \mathcal{M}_0\mathcal{M}_1$ with $\mathcal{M}_{1,2}^2 = \mathrm{Id}$, establishing reversibility of $\mathcal{M}$, *i.e.* $\mathcal{M}^{-1} = \mathcal{M}_1\mathcal{M}_0$. The map $\mathcal{M}_0$ is given by

$$\bar{x}^{(k)} = x^{(2N-1+k)}, \qquad 1 \leq k \leq 2N, \tag{11}$$

and $\mathcal{M}_1$ reads as

$$\bar{x}^{(k)} = x^{(2N-k)}, \qquad 1 \leq k \leq 2N-1$$

$$\bar{x}^{(2N)} = \frac{1}{V_N}\left[\omega x^{(N)} - \gamma (x^{(N)})^3 - \sum_{m=1}^{N} V_m \left(x^{(N+m)} + x^{(N-m)}\right)\right] - x^{(2N)}.$$

We focus interest on the excitation of localized states on the lattice. Lead by our experiences from the planar case ($N = 1$) we note that such localized stationary solutions correspond to map orbits lying on the stable and unstable manifolds of hyperbolic equilibria [22]. If, in particular, the map origin represents an unstable hyperbolic equilibrium point then a bright solitonlike solution provided by the corresponding homoclinic map orbit is excitable. As it is apparent from the system (9, 10) the origin represents an equilibrium point of the map $\mathcal{M}$. Its spectral stability can determined by the solution properties of the characteristic polynomial $\det(D\mathcal{M} - \lambda I) = 0$ associated with the tangent map at the origin which reads as

$$\lambda^{2N} - \frac{\omega}{V_N}\lambda^N + \frac{1}{V_N}\sum_{m=1}^{N-1} V_m(\lambda^{N-m} + \lambda^{N+m}) + 1 = 0 \quad \text{and} \quad V_N \neq 0, \quad N \geq 2. \tag{12}$$

Since the characteristic polynomial is reflexive, it follows that complex eigenvalues occur generally in $2N$-tuples $(\lambda_k, \lambda_k^{-1}, \lambda_k^*, \lambda_k^{*-1})$ with $1 \leq k \leq N$. If all $|\lambda_k| = 1$ then they occur in complex conjugate pairs while real eigenvalues come in pairs $(\lambda_k, \lambda_k^{-1})$. In the latter case the equilibrium point is unstable having $N$-dimensional stable and unstable manifolds in the $2N$-dimensional phase space. To visualize these manifolds we use two-dimensional projections on the various $x^{(i)}$–$x^{(j)}$-hyper planes with $i \neq j$. Due to the reversibility property $\phi_n \longleftrightarrow \phi_{n-1}$ it follows that the map obeys the reflection symmetry $x^{(k)} \longleftrightarrow x^{(k+1)}$ for $1 \leq k \leq 2N-1$. Exploiting this symmetry it can be readily shown that for a proper projection of the invariant manifolds it suffices to consider only the plane of neighboring amplitudes $x^{(k)} - x^{(k+1)}$ for one given $k$.

In order to illustrate the excitation of localized solutions based on the homoclinic orbit in a phase space of dimension larger than two, we consider the case $N = 2$ yielding a four-dimensional map. In principle this analysis can be extended to any dimension. We only have to solve the characteristic equation (12). However, the computations become rather lengthy and tedious with increasing dimension so that we restrict ourselves here to $N = 2$ to compare with the results of stationary analysis in the planar case [21]. The roots of the characteristic polynomial assigned to the equilibrium of the map origin are computed as

$$\lambda = \frac{1}{2}\left(\rho \pm \sqrt{\rho^2 - 4}\right), \tag{13}$$

with

$$\rho = \frac{1}{2}\left(-\frac{V_1}{V_2} \pm \sqrt{\left(\frac{V_1}{V_2}\right)^2 + \frac{4\omega}{V_2} + 8}\right). \tag{14}$$

If the condition $|\rho| > 2$ is fulfilled then there exist real eigenvalues $\lambda$ and the origin $(0,0,0,0)$ represents an unstable hyperbolic point. From equation (14) we infer that for $\rho > 2$ it must hold that

$$\omega > 2(V_1 + V_2), \tag{15}$$

while for $\rho < -2$ we get the condition

$$\omega < -2(V_1 + V_2). \tag{16}$$

From the dispersion relation of the linear lattice equation ($\gamma = 0$) we derive that the linear band is constrained by the inequality

$$-2(V_1 + V_2) \leq \omega \leq 2(V_1 + V_2). \tag{17}$$

Thus the conditions (15) respectively (16) tell us actually that in order to get localized lattice solutions (linked with a hyperbolic orbit of the unstable fixed point of the map origin) the frequency $\omega$ has to lie above respectively below the linear band. Therefore for positive (negative) frequencies $\omega > 0$ ($\omega < 0$) the localized solutions appear as unstaggered (staggered) solitons [26]. This has to be distinguished from the localization properties of the standard DNLS for positive nonlinearity strength $\gamma > 0$ as well as positive coupling constant $V_1 > 0$ for which localization is possible only if the frequency $\omega$ lies above the linear band [21], that is $\omega > 2V_1$. In this case the soliton-like states are of unstaggering nature [26]. Interestingly, taking into account the n-n-n interaction besides the positive-frequency unstaggered localized states also staggered soliton-like states whose amplitudes oscillate with negative frequency occur. This result is in accordance with the findings of the modulational instability analysis (see Fig. 1b).

To depict the homoclinic tangle of the invariant manifolds of the hyperbolic point we approximate the stable, respectively, the unstable, manifold in the vicinity of the hyperbolic point by the linear subspaces (straight lines in the direction of the eigenvectors) of the tangent map. After iteration of a few thousand points on them several times we obtain the homoclinic tangle. In Figure 3 we plot the projections of the four-dimensional stable and unstable manifold of the hyperbolic equilibrium on the $x^{(1)}$–$x^{(2)}$-plane for the parameters $\gamma = 1$, $V_1 = 0.2$ and $V_2 = 0.01$. The manifolds extending along the linear eigenspaces belonging to the positive eigenvalue pair $(\lambda_1, \lambda_1^{-1})$ $((\lambda_2, \lambda_2^{-1}))$ obtained for $\omega = 0.9$ ($\omega = -0.9$) are drawn in Figure 3a (3b). One infers that there exist transversal intersections of the stable and unstable manifolds at isolated points forming homoclinic orbits $\{\phi_n^{\rm hom}\}$. Apparently, the windings as well as the location of the first intersection points of the manifolds corresponding to the negative eigenvalues $(\lambda_2, \lambda_2^{-1})$ expand much more towards larger $|x|, |y|$ as in the case of the positive $(\lambda_1, \lambda_1^{-1})$. However, with regard to the amplitude pattern $|c_n(t)|^2$ it makes no difference whether the solitons are of staggering or unstaggering type. Hence, the staggered solitonic state possesses a much larger peak height than the unstaggered one.

How the homoclinic connections can be exploited to construct standing solitonlike solutions of lattice chains has been shown *e.g.* in [21]. To this end we use the fact that the homoclinic points approach the origin asymptotically along the stable (unstable) manifold for $n \to \infty$ $(-\infty)$, respectively. Therefore, each homoclinic orbit $\{\phi_n^{\rm hom}\}$ is attributed to a localized state pinned by the lattice. Figure 4 shows the profile of stationary solitonlike excitations $|c_n|^2$ of the DNLS lattice with different $V_2$. We conclude that the DNLS lattice of n-n-n interaction radius bears stationary localized states of amplitudes smaller than the ones for the standard DNLS solitons and with increasing transfer matrix element $V_2$ the soliton peak height reduces further. The positive real eigenvalues $\lambda_1$ diminish monotonically with increasing $V_2$ and obey further the inequal-

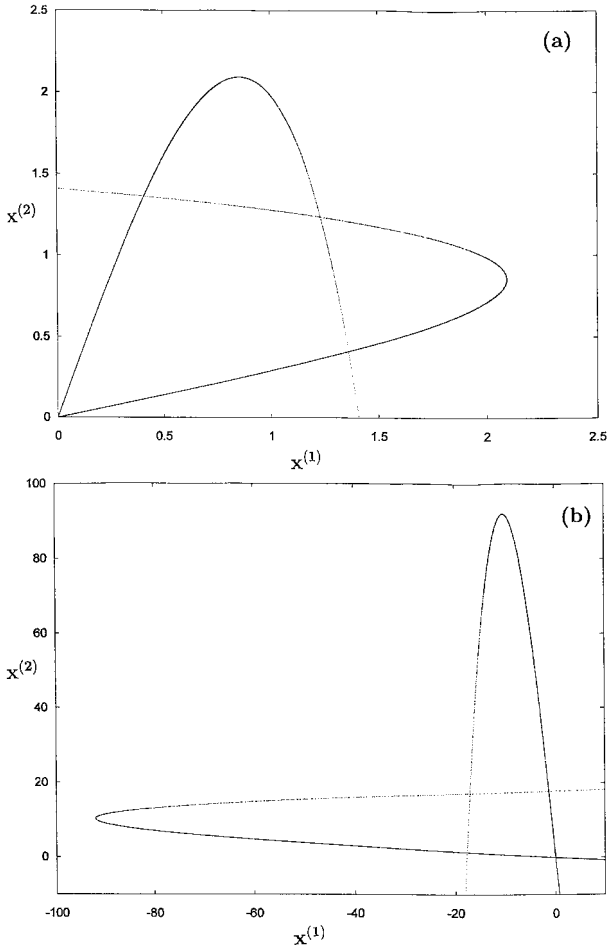


**Fig. 3.** Two-dimensional projections of the four-dimensional homoclinic tangle of the hyperbolic point $(0, 0, 0, 0)$ on the $x^{(1)}$–$x^{(2)}$-plane. The parameters are $\gamma = 1$, $V_1 = 0.2$ and $V_2 = 0.01$. (a) The first windings of the manifolds corresponding to the pair of positive eigenvalues $(\lambda_1, \lambda_1^{-1})$ occurring for positive frequency $\omega = 0.9$. (b) As in (a) for the pair of negative eigenvalues $(\lambda_2, \lambda_2^{-1})$ with $\omega = -0.9$.

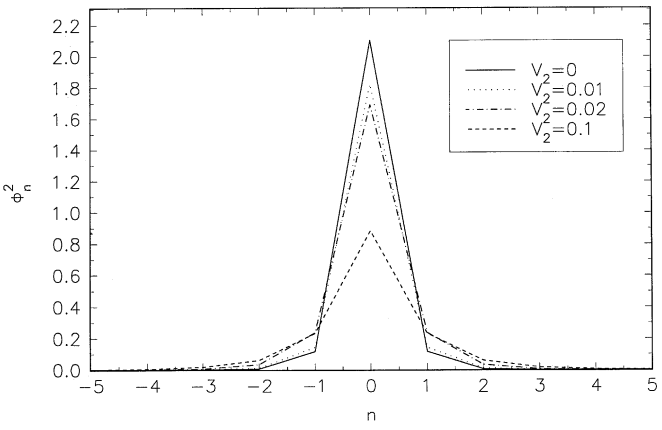


**Fig. 4.** The amplitude profile of the stationary soliton-like states of the n-n-n DNLS lattice of equation (1) with $N = 2$. The amplitudes of the stationary solitonlike solutions are gained from the homoclinic map orbits. Parameters as in Figure 3a except for the different $V_2$ as indicated.

ity $\lambda_1 \leq \tilde{\lambda}$, where $\tilde{\lambda}$ is the maximal eigenvalue related to the unstable zero equilibrium point of the planar map of $N = 1$. Therefore we infer that the larger the relative interaction strength $V_2/V_1$ the less rapid is the decay of the soliton tails due to $|c_n| \sim |\lambda|^{|n|}$ which is clearly seen in Figure 4.

The linear stability of the localized solutions is proven in a standard way with the help of the Floquet theory [29]. To investigate the linear stability of a time-periodic localized state $c_n^{(0)}(t) = \phi_n^{\mathrm{hom}} \exp(\mathrm{i}\omega t)$ we make the ansatz $c_n(t) = [\phi_n + \delta c_n(t)] \exp(\mathrm{i}\omega t)$ including a small perturbation $\delta c_n(t)$. Linearizing around $c_n = \phi_n$ gives the linear system of tangent equations for $\delta c_n(t)$

$$\begin{aligned}\mathrm{i}\,\delta\dot{c}_n = (\omega - 2\gamma\phi_n^2)\delta c_n - \gamma\phi_n^2\delta c_n^* \\ -V_1(\delta c_{n+1} + \delta c_{n-1}) - V_2\,(\delta c_{n+2} + \delta c_{n-2}). \quad (18)\end{aligned}$$

Decomposing into real and imaginary parts, $\delta c_n = a_n + \mathrm{i}b_n$ we obtain eventually

$$\begin{aligned}\dot{a}_n = \left[\,\omega - \gamma\phi_n^2\,\right]\, b_n - V_1\,(b_{n+1} + b_{n-1}) \\ -\,V_2\,(b_{n+2} + b_{n-2}), \quad (19)\end{aligned}$$

$$\begin{aligned}\dot{b}_n = -\left[\,\omega + 3\gamma\phi_n^2\,\right]\, a_n + V_1\,(a_{n+1} + a_{n-1}) \\ +\,V_2\,(a_{n+2} + a_{n-2}). \quad (20)\end{aligned}$$

Integrating the tangent equations (19) and (20) over one period $T = 2\pi/\omega$ yields a linear map

$$\begin{pmatrix} a_n(T) \\ b_n(T) \end{pmatrix} = F \begin{pmatrix} a_n(0) \\ b_n(0) \end{pmatrix}, \quad (21)$$

where $F$ is the Floquet matrix. Linear stability of the solution $c_n^{(0)}(t)$ requires that all eigenvalues of the matrix $F$ are situated on the unit circle; otherwise the solution will be linearly unstable. We have proven numerically that the Floquet eigenvalues stay on the unit circle ensuring linear stability for the stationary localized solutions derived from the homoclinic map orbit.

The decreasing height and increasing width of the standing soliton-like states with enlarged $V_2$ seems to be in contradiction to the findings for the modulational instability analysis where the spontaneous formation of multiple localized pulses due to modulational instability of plane wave solutions suggests an opposite tendency. However, these localized multi-pulse states do not represent rigorous solutions of the nonintegrable DNLS lattice. They are rather sensitive with respect to perturbations whereas the standing soliton-like states derived from the stationary map constitute exact stable nonlinear localized eigenstates of the DNLS lattice which are robust under linear perturbations.

Finally, we remark that the map approach for the construction of solitonlike solutions can also be invoked if the range of the interaction is extended for $N > 2$. The only difference lies in the consideration of a then higher dimensional map making the existence of homoclinic orbits of number $2N \geq 2$ possible.

## 4 Summary and conclusions

In this paper we considered a DNLS with n-n-n interaction. We focused interest on the creation of intrinsically localized modes. To this aim the first part of the paper dealt with the formation of localized pulses due to modulational instability. We identified regions in parameter space for which the perturbations of plane wave solutions result in localized solutions. The most striking feature is that also high-frequency carrier waves exhibit modulational instability for n-n-n interaction so that two types of localized pulses occur for which neighboring lattice oscillators perform in-phase respectively out-of-phase motion. Furthermore it was found that the lower the interaction ratio $V_1/V_2$ the stronger localized are the pulses, meaning that not only their amplitudes grow but also their widths diminish. The spontaneous adaptation to intensified degree of localization is the inherent mechanism of the lattice system to maintain its localized structures and to protect them against the increased dispersion.

The second part of the paper presented an approach to construct exact localized states of the n-n-n interaction DNLS utilizing a nonlinear map. The dimension of this map is directly determined by the number of sites encompassed by the interaction radius. Parameter constellations such that the map origin represents an unstable hyperbolic equilibrium were identified. The corresponding homoclinic orbits were used to excite stationary solitonlike lattice states the stability of which was readily shown by Floquet theory. Interestingly, the n-n-n DNLS supports two types of standing solitons, namely staggered as well as unstaggered ones. This variety of solutions does not appear for the stationary system of the standard DNLS for which the single stationary localized state is depending on the relative signs of the nonlinearity parameter and the transfer matrix element either of staggering or unstaggering nature. With view to the localization properties of polymer chains the n-n-n DNLS-model provides bistable localized states to which excitation patterns of different amplitude height and localization strength can be targeted to. Moreover, one can take advantage of this multistability property and construct a switching mechanism accomplishing the controlled transition between the two stationary localized states similar to the procedure used in [9].

This work was supported by the Deutsche Forschungsgemeinschaft *via* the Heisenberg-program (He 3049/1-1).

## References

1. see *e.g.* T. Holstein, Ann. Phys. (N.Y.) **8**, 325 (1959); A.S. Davydov, J. Theor. Biol. **38**, 559 (1973); J.C. Eilbeck, P.S. Lomdahl, A.C. Scott, Physica D **16**, 318 (1985); D.N. Christodoulides, R.I. Joseph, Optics Letters **13**, 794 (1988); N. Finlayson, G.I. Stegeman, Appl. Phys. Lett. **56**, 2276 (1990); Y. Chen, A.W. Snyder, D.J. Mitchell, Electron. Lett. **26**, 77 (1990); H. Feddersen, P.L. Christiansen, M. Salerno, Physica Scripta **43**, 353 (1991).

2. A.S. Davydov, *Solitons in Molecular Systems* (D. Reidel, Dordrecht, Boston, Lancaster, 1985).
3. A.C. Scott, Phys. Rep. **217**, 1 (1992).
4. J.A. McCammon, S.C. Harvey, *Dynamics of Proteins and Nucleic Acids* (University Press, Cambridge, UK, 1987).
5. Yu.B. Gaididei, N. Flytzanis, A. Neuper, F.G. Mertens, Phys. Rev. Lett. **75**, 2240 (1995).
6. Yu.B. Gaididei, S.F. Mingaleev, P.L. Christiansen, K.Ø. Rasmussen, Phys. Rev. E **55**, 6141 (1997).
7. Y. Ishimori, Progr. Theor. Phys. **68**, 402 (1982).
8. M. Remoissenet, N. Flytzanis, J. Phys. C **18**, 1573 (1985).
9. M. Johansson, Yu.B. Gaididei, P.L. Christiansen, K.Ø. Rasmussen, Phys. Rev. E **57**, 4739 (1998).
10. P.L. Christiansen, Yu.B. Gaididei, M. Johansson, K.Ø. Rasmussen, V.K. Mezentsev, J.J. Rasmussen, Phys. Rev. B **57**, 11303 (1998).
11. S. Flach, Phys. Rev. E **58**, R 4116 (1998); Physica D **113**, 184 (1998).
12. D. Bonart, T. Rössler, J.B. Page, Physica D **113**, 123 (1998).
13. S.F. Mingaleev, Yu.B. Gaididei, F.G. Mertens, Phys. Rev. E **61**, R 1044 (2000).
14. R.S. MacKay, S. Aubry, Nonlinearity **7**, 1623 (1994).
15. M. Johansson, S. Aubry, Nonlinearity **10**, 1151 (1997).
16. S. Flach, C.R. Willis, Phys. Rep. **295**, 181 (1998).
17. S. Takeno, J. Phys. Soc. Jpn **58**, 759 (1989).
18. R. Scharf, A.R. Bishop, Phys. Rev. A **43**, 6535 (1991).
19. Yu.S. Kivshar, D.K. Campbell, Phys. Rev. E **48**, 3077 (1993); Yu.S. Kivshar, Phys. Rev. Lett. **70**, 3055 (1993).
20. D. Cai, A.R. Bishop, N. Grønbech Jensen, Phys. Rev. E **52**, 5784 (1995); Phys. Rev. E **53**, 4131 (1996).
21. D. Hennig, K.Ø. Rasmussen, H. Gabriel, A. Bülow, Phys. Rev. E **54**, 5788 (1997).
22. D. Hennig, G.P. Tsironis, Phys. Rep. **307**, 333 (1999).
23. Yu.S. Kivshar, M. Peyrard, Phys. Rev. A **46**, 3198 (1992).
24. D.W. McLaughlin, C.M. Schober, Physica D **57**, 447 (1992).
25. Yu.S. Kivshar, Phys. Rev. E **48**, 4132 (1993).
26. D. Cai, A.R. Bishop, N. Grønbech Jensen, Phys. Rev. Lett. **72**, 591 (1994).
27. Yu.S. Kivshar, M. Salerno, Phys. Rev. E **49**, 3543 (1994).
28. M. Remoissenet, *Waves Called Solitons* (Springer-Verlag, Berlin, 1978).
29. S. Aubry, Physica D **103**, 1 (1997).